Asian Journal of Pharmaceutical Sciences 13 (2018) 450–458

Available online at www.sciencedirect.com

ScienceDirect

journal homepage: www.elsevier.com/locate/AJPS

Original Research Paper

Design and characterization of clindamycin-loaded nanofiber patches composed of polyvinyl alcohol and tamarind seed gum and fabricated by electrohydrodynamic atomization

Tanikan Sangnim[a], *Sontaya Limmatvapirat*[b,c], *Jurairat Nunthanid*[b,c], *Pornsak Sriamornsak*[b,c], *Wancheng Sittikijyothin*[d], *Sumalee Wannachaiyasit*[a], *Kampanart Huanbutta*[a,*]

[a] *Faculty of Pharmaceutical Sciences, Burapha University, Chonburi 20131, Thailand*
[b] *Department of Pharmaceutical Technology, Faculty of Pharmacy, Silpakorn University, Nakhon Pathom 73000, Thailand*
[c] *Pharmaceutical Biopolymer Group (PBiG), Faculty of Pharmacy, Silpakorn University, Nakhon Pathom 73000, Thailand*
[d] *Department of Chemical Engineering, Faculty of Engineering, Burapha University, Chonburi 20131, Thailand*

ARTICLE INFO

Article history:
Received 28 October 2017
Accepted 9 January 2018
Available online 31 January 2018

Keywords:
Electrohydrodynamic atomization (EHDA)
Polymeric nanofiber
Clindamycin
Wound dressing

ABSTRACT

In this study, we developed a polymeric nanofiber patch (PNP) for topical disease treatment using electrohydrodynamic atomization (EHDA). The nanofibers were prepared using various concentrations of polyvinyl alcohol (PVA) and tamarind seed gum and loaded with clindamycin HCl as a model drug. The precursor polymer solutions were sprayed using the EHDA technique; the EHDA processing parameters were optimized to obtain blank and drug-loaded PNPs. The skin adherence, translucence, and ventilation properties of the prepared PNPs indicated that they are appropriate for topical application. The conductivity of the polymer solution increased with increasing PVA and clindamycin concentrations, and increasing the PVA concentration enhanced the solution viscosity. Based on scanning electron microscopy analysis, the PVA concentration had a pronounced effect on the morphology of the sprayed product. Nanofibers were fabricated successfully when the solution PVA concentration was 10%, 13%, or 15% (w/v). The applied voltage significantly affected the diameters of the prepared nanofibers, and the minimum nanofiber diameter was 163.86 nm. Differential scanning calorimetry and X-ray diffraction analyses indicated that the model

* Corresponding author. Faculty of Pharmaceutical Sciences, Burapha University, Chonburi, 20131, Thailand. Tel.: +66 38 102610.
E-mail address: kampanart@go.buu.ac.th (K. Huanbutta).
Peer review under responsibility of Shenyang Pharmaceutical University.

https://doi.org/10.1016/j.ajps.2018.01.002

drug was dispersed in PVA in an amorphous form. The PNP prepared with a PVA:gum ratio of 9:1 absorbed water better than the PVA-only PNP and the PNP with a PVA:gum ratio of 9.5:0.5. Moreover, the PNPs loaded with clindamycin at concentrations of 1%–3% prohibited the growth of *Staphylococcus aureus* more effectively than clindamycin gel, a commercially available product.

1. Introduction

Acne vulgaris is a chronic inflammatory disease of the pilosebaceous unit that results in the formation of comedones, inflammatory papules, pustules, nodules, cysts, and scars. Acne vulgaris primarily manifests in the face and trunk and most commonly presents during puberty [1]. This skin disease represents a significant health burden in the United States, with 40–50 million general practice consultations for acne [2]. Several types of topical treatments have been developed for acne vulgaris, including solutions, gels, creams, and hydrogels [3,4]. However, each of these dosage forms has limitations. For example, topical solutions do not remain at the site of application for sufficient time periods, and the treatment solution can be lost or contaminated during use. Hydrogels leave a visible polymer stain on the face after drying, while cream and hydrogel films impede skin ventilation, affecting the healing process [5].

Based on these drawbacks of conventional topical formulations, several alternative treatment modalities have been developed, including polymeric micellar nanocarriers [6] and solid lipid nanoparticles [7,8]. Among the various new approaches, polymeric nanofiber patches (PNPs) have evolved as an alternative remedy for acne vulgaris because of their numerous advantages, such as high ratio of surface area to volume, skin concealment, high porosity, fine pores, and aspect ratio. These properties make non-woven mats composed of nanofiber patches excellent candidates for various applications, including the treatment of acne, wound dressing, and drug delivery.

Electrohydrodynamic atomization (EHDA), in which an external electric field is imposed on a polymer solution or melt, is a promising technique for producing continuous polymer fibers with nanoscale diameters [9,10]. In theory, during EHDA, a liquid breaks up into droplets under the drive of an electric field. Various modes of EHDA have been reported; in this study, the stable cone-jet method is of specific interest [11]. In this mode, a liquid flowing through a nozzle is maintained at high potential and subjected to an electric field (Fig. 1), leading to the elongation of the meniscus and the formation of a jet. Subsequently, the jet deforms and breaks up into fine droplets. The small jet diameter allows rapid solvent evaporation, causing the particles to be deposited on the collector. Various process parameters (i.e., applied voltage, feed rate, distance between the nozzle and collector, drum collector rolling rate, and charge and viscosity of the sprayed solution) significantly affect the characteristics of products produced using EHDA [11].

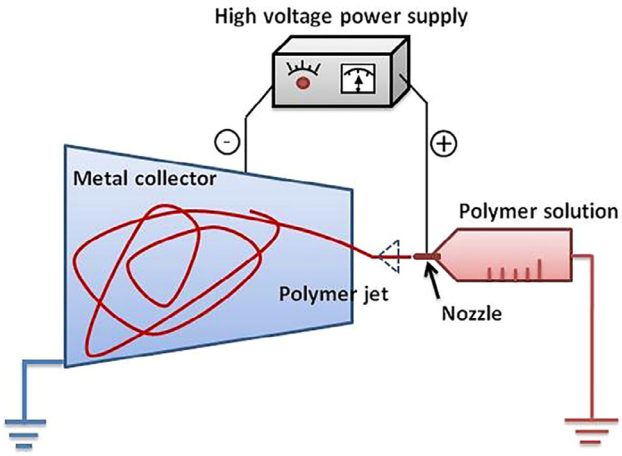

Fig. 1 – Schematic diagram of nanofiber fabrication using EHDA.

For drug-delivery systems, the principal advantages of EHDA are that it provides (i) the opportunity for heat-sensitive drug loading, (ii) a relatively rapid and simple way to combine several materials into nanoparticles, and (iii) controllable operation factors.

In this study, polyvinyl alcohol (PVA), a water-soluble synthetic polymer, and carboxymethylated gum prepared from tamarind (*Tamarindus indica*) seed were utilized to fabricate PNPs because of their low toxicity, biodegradability, bioadhesive nature, and biocompatibility [12,13]. Clindamycin, an effective antibacterial agent that is commonly used to treat acne vulgaris, was selected as the model drug [4].

The objective of this paper is to fabricate and characterize clindamycin-loaded PVA/gum nanofiber acne patches using EHDA. The effects of EHDA parameters (applied voltage, injection distance, feed rate, and drum collector rolling rate) on the physiochemical properties of the products were carefully examined. Finally, the antimicrobial activity of the drug-loaded PVA/gum PNP was evaluated and compared to that of a commercially available acne treatment.

2. Materials and methods

2.1. Materials

PVA (batch number 02628LD) was purchased from Sigma-Aldrich. Clindamycin hydrochloride (lot number 27058) was a

gift from Bangkok Lab & Cosmetic Co., Ltd., Thailand. Crude gums were obtained from *T. indica* (gum) seeds collected in Uthai Thani province in Thailand. Clindamycin gel (Clindalin gel®; batch number 106110) was purchased from Union Drug Laboratories, Ltd. All other chemicals were of reagent grade and used without further purification.

2.2. Carboxymethylated gum preparation

Carboxymethylated gum was prepared using the method presented in our previous paper [14] with some modification. The reaction was conducted at 70 °C for 1 h with ethanol as the solvent. Different molar ratios of sodium hydroxide (NaOH) to monochloroacetic acid ($ClCH_2COOH$) were used. The amount of crude gum from the seed of *T. indica* was 0.56 mol in all cases. The reaction product was precipitated and washed with ethanol to remove ionic salts. The carboxymethylated gum was removed by filtration and washed with 80% ethanol. Finally, the washed product was dried at 40 °C for 4 h. The degrees of substitution of the carboxymethylated gums were determined as follows [15]:

$$W_A = \frac{C_{NaOH}V_{NaOH} - C_{HCl}V_{HCl}}{m}, \text{ and} \quad (1)$$

$$DS = \frac{162W_A}{58(100 - W_A)}, \quad (2)$$

where W_A is the mass fraction of the acetyl groups; C_{NaOH} and C_{HCl} are the molar concentrations of the standard NaOH and HCl solutions, respectively; V_{NaOH} and V_{HCl} are the volumes of the standard NaOH and HCl solutions, respectively; m is the weight of the sample; and 58 and 162 are the molar masses (g/mol) of the acetyl group and anhydroglucose unit, respectively.

2.3. Characterization of the polymer solution

The prepared polymer (PVA and/or gum) solutions were characterized to evaluate the effects of the polymer solution properties on the resultant nanoparticles. The conductivity of each solution was measured using a conductivity meter (model ECtestr11+, Eutech Instruments Pte Ltd., Singapore), and the viscosity was evaluated using a viscometer (model DV-III Ultra, Brookfield, USA). The surface tension was measured with a surface tensiometer (k20s Easydyne, Krüss, Germany). All experiments were performed in triplicate.

2.4. PNP preparation

To prepare blank PNPs, various amounts of PVA, gum, and clindamycin were dissolved in 100 ml purified water (Table 1). Each polymer solution was then sprayed using an EHDA instrument (Bangkok Cryptography, Thailand). The processing parameters (applied voltage, injection distance, feed rate, and drum collector rolling rate) were carefully adjusted to obtain blank and drug-loaded PNPs. All products were stored in a desiccator for further investigation.

Table 1 – PNP formulations.

Formulation	PVA (g)	Gum (g)	Clindamycin (g)
1	3	–	–
2	5	–	–
3	10	–	–
4.1	9.5	0.5	–
4.2	9.5	0.5	1
4.3	9.5	0.5	1.5
4.5	9.5	0.5	2
4.5	9.5	0.5	2.5
5.1	9	1	–
5.2	9	1	1
5.3	9	1	1.5
5.4	9	1	2
5.5	9	1	2.5
6	8	2	–
7	6	4	–
8	6.66	3.33	–
9	5	5	–

2.5. PNP appearance and morphology

The physical appearances of the PNPs were observed using a digital camera, while the surface morphologies were evaluated by scanning electron microscopy (SEM; model Maxim 2000S, CamScan Analytical, UK). The samples for SEM analyses were pasted on stubs and sputter-coated with gold to increase their conductance. Fiber diameter was analyzed by J MicroVision software (version 1.2.7).

2.6. Fourier transform infrared (FTIR) spectroscopy

To investigate the effects of the EHDA processing parameters on the drug–polymer interactions, PVA, gum, clindamycin, their physical mixtures, and the clindamycin-loaded PNP with a PVA:gum:clindamycin ratio of 9:1:1 were pulverized and blended with KBr and then compressed. The pellets were then analyzed using an FTIR spectrophotometer (model Magna-IR system 750, Nicolet Biomedical Inc., USA).

2.7. Powder X-ray diffraction

The powder X-ray diffraction patterns of the starting materials, their physical mixtures, and the PNP with a PVA:gum:clindamycin ratio of 9:1:1 were obtained using a powder X-ray diffractometer (model D8, Bruker, Germany) under the following conditions: graphite monochromatized Cu Kα radiation, voltage = 45 kV, electric current = 40 mA, slit: DS1°, SS1°, RS 0.15 nm, and scanning ratio $2\theta = 5°$/min.

2.8. Differential scanning calorimetry (DSC)

The DSC thermograms of the starting materials, their physical mixtures, and the PNP with a PVA:gum:clindamycin ratio of 9:1:1 were measured using a differential scanning calorimeter (model Sapphire, Perkin Elmer, USA) with indium as a standard. Each sample (2–3 mg) was weighed into a solid aluminum pan. The temperature was increased from 20 °C to 300 °C at 10 °C/min under nitrogen.

2.9. Liquid absorption

The liquid-absorbing abilities of the samples were studied in distilled water at 25 °C ± 2 °C by placing a sample of known weight in water for 30 sec. Subsequently, the excess water was gently removed with tissue paper, and the wet sample was weighed. The percentage of liquid absorption was determined as:

$$\text{liquid absorption (\%)} = \frac{W_s - W_d}{W_d} \times 100, \quad (3)$$

where W_d and W_s are the weights of the dry and wet samples, respectively.

2.10. Antimicrobial studies

A disk-diffusion method was used to assay drug-loaded PNPs for bactericidal activity against test strains on Müller–Hinton agar (MHA) plates. To prepare the MHA plates, 0.1 ml of *Staphylococcus aureus* or *Propionibacterium acnes* was transferred into 10 mL Trypticase soy broth and then inoculated at 37 °C for 18–24 h (medium1). The prepared solution (medium1) was pipetted into 0.9% sterile normal saline solution in which the amount of organism suspension was equivalent to 0.5 McFarland (medium 2). Sterile cotton was dipped into medium 2 and swabbed onto the MHA plates. To determine the antibacterial efficiency of the PNP formulation, a standard paper disk was also impregnated with 10 μl of 0.1% clindamycin solution. The freshly prepared PNP with a final content of approximately 10 μg/patch and the paper disk containing dispersed commercial clindamycin gel (10 μg/disk) were evaluated for antimicrobial activity. The erythromycin disk and a blank disk were used as the positive and negative controls, respectively. The zone of strain inhibition was recorded after 16–18 h of incubation at 35 °C. Each test was conducted five times.

2.11. Statistical analysis

Analysis of variance (ANOVA) and Levene's test for homogeneity of variance were performed using SPSS version 10.0 for Windows (SPSS Inc., USA). The multiple comparisons were subjected to post hoc testing ($P < 0.05$) using either the Scheffé or Games–Howell test (for when Levene's test was insignificant or significant, respectively).

3. Results and discussion

3.1. Characterization of the polymer solution

Before the EHDA process, the polymer solutions were characterized to evaluate the effects of solution properties on the appearance of the products. As illustrated in Fig. 2 , the viscosity of the spraying solution depended strongly on PVA concentration; viscosity increased dramatically with increasing PVA concentration.

The conductivity and surface tension of each polymer solution are shown in Table 2. The solution conductivity increased with increasing PVA concentration from 13% to 15%. However, the surface tension was not affected by PVA concentration,

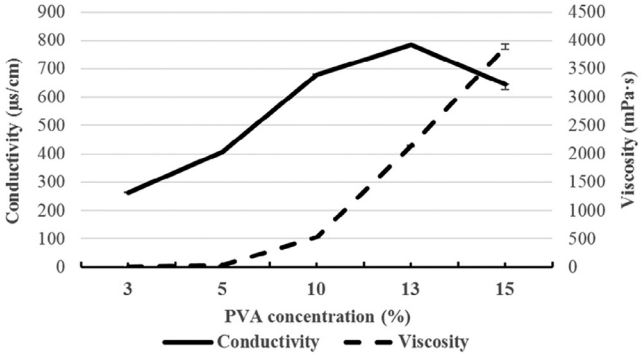

Fig. 2 – Conductivity and viscosity of the EHDA spraying solution as functions of PVA concentration.

which agrees with our previous finding that surface tension depends on the solvent type rather than the PVA concentration [16]. Tamarind seed gum is an ionized polymer in aqueous solution and has the ability to alter solution properties; in this study, the addition of gum increased both the conductivity and surface tension. Finally, the solution conductivity increased significantly with increasing clindamycin content because the hydrochloride form of clindamycin was protonated in the aqueous solution, resulting in higher conductivity [17].

3.2. Physical appearance and morphology

Images of the PNP with a PVA:gum ratio of 9:1 and loaded with 1% clindamycin HCl are shown in Fig. 3 . The prepared thin film-like PNP, which was white in appearance (Fig. 3A), could be closely attached to the skin (Fig. 3B) and became transparent when the skin was moist (Fig. 3C).

SEM images of the PVA nanofibers prepared from different polymer solutions are shown in Fig. 4 . The fibers prepared from solutions containing 3% and 5% PVA were disconnected and contained beads (Fig. 4A and B). Continuous fibers without beads were obtained when the PVA concentration was between 10% and 15% (Fig. 4C–E). The average diameters of the fibers fabricated from solutions containing 10%, 12%, and 15% PVA were 216.67 nm ± 26.85%, 244.66 nm ± 20.43%, and 260.39 nm ±14.25%, respectively. Thus, with increasing PVA concentration, the fiber diameter increased slightly, whereas the relative standard deviation decreased. This phenomenon can be explained by the whipping model, which indicates that the diameter depends on the flow rate, electric current, and surface tension [18,19]:

$$h_t = c(I/Q)^{-2/3}\gamma^{1/3}, \quad (4)$$

where c is a constant, h_t is the dimensionless conductivity of the fluid, I is the electric current, Q is the constant volume flow rate, and γ is the surface tension.

SEM images of the PNPs fabricated at different applied voltages are shown in Fig. 5 . The average diameters of the fibers formed at applied voltages of 5, 10, 15, 20, and 25 kV were 260.02 nm ± 22.62%, 233.73 nm ± 19.01%, 172.89 nm ± 26.34%, 163.86 nm ± 26.93%, and 186.65 nm ± 23.50%, respectively. Thus, the fiber diameter decreased as applied voltage increased from 5 to 20 kV; however, further increase in the

Table 2 – Conductivity, viscosity, and surface tension of the PVA solutions and diameter of the corresponding nanofiber.

PNP formulation			Properties of the spraying formulation		Diameter of the prepared nanofiber (nm)
PVA conc. (%w/w)	Gum (%w/w)	Clindamycin (%w/w)	Conductivity (μs/cm)	Surface tension (mN/m)	
3	–	–	264.00 ± 1.00	45.45 ± 0.35	NA
5	–	–	406.67 ± 0.58	44.68 ± 0.42	NA
10	–	–	679.33 ± 2.52	45.23 ± 0.26	216.67 ± 26.85%[a]
13	–	–	782.67 ± 3.51	46.73 ± 0.89	244.66 ± 20.43%[a]
15	–	–	645.00 ± 18.03	46.28 ± 0.60	260.39 ± 14.25%[a]
10	2.5	–	1139 ± 6.24	46.17 ± 0.29	
10	5.0	–	1399 ± 9.17	50.63 ± 1.15	
10	7.5	–	1619 ± 27.74	53.47 ± 0.64	
5	–	1	554.00 ± 1.73	42.18 ± 0.19	NA
5	–	1.5	591.67 ± 0.58	42.66 ± 1.52	NA
5	–	2	592.33 ± 1.53	43.08 ± 0.44	NA
5	–	2.5	628.33 ± 4.51	42.94 ± 0.44	NA
10	–	1	849.67 ± 7.09	45.00 ± 1.22	277.80 ± 27.05%[b]
10	–	1.5	934.67 ± 3.51	45.72 ± 0.59	263.24 ± 20.84%[b]
10	–	2	981.00 ± 2.65	45.78 ± 0.48	234.73 ± 20.84%[b]
10	–	2.5	1047.67 ± 2.52	46.12 ± 0.49	202.65 ± 26.45%[b]

NA: Diameter could not be measured because the product was not in the shape of a fiber.
[a] Applied voltage was 15 kV.
[b] Applied voltage was 20 kV.

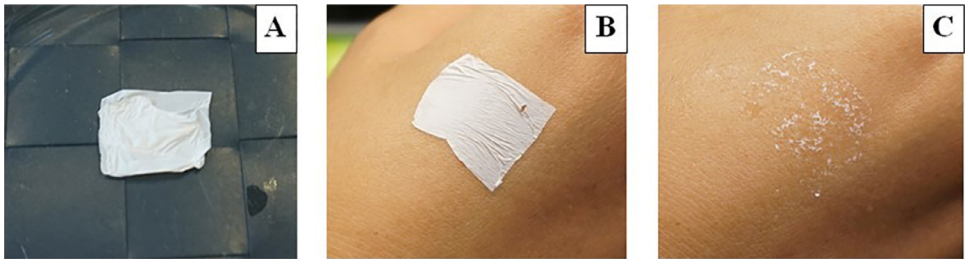

Fig. 3 – Physical appearance of the PNP with a PVA:gum ratio of 9:1 and loaded with 1% clindamycin HCl: (A) after preparation and when placed on (B) dry skin and (C) moist skin.

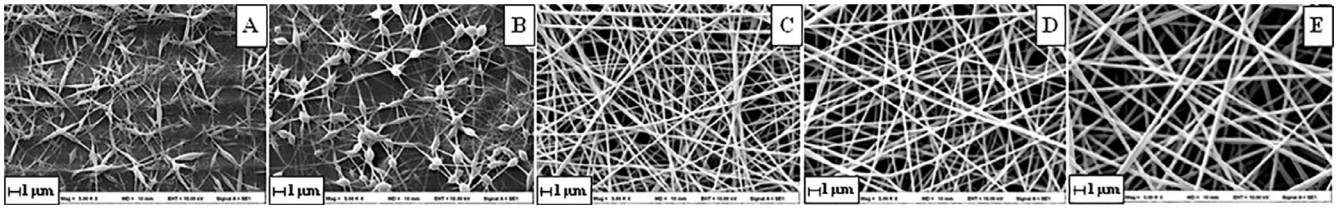

Fig. 4 – SEM images of the nanofibers prepared from solutions containing (A) 3%, (B) 5%, (C) 10%, (D) 13%, and (E) 15% (w/w) PVA (applied voltage is 15 kV; injection distance is 20 cm).

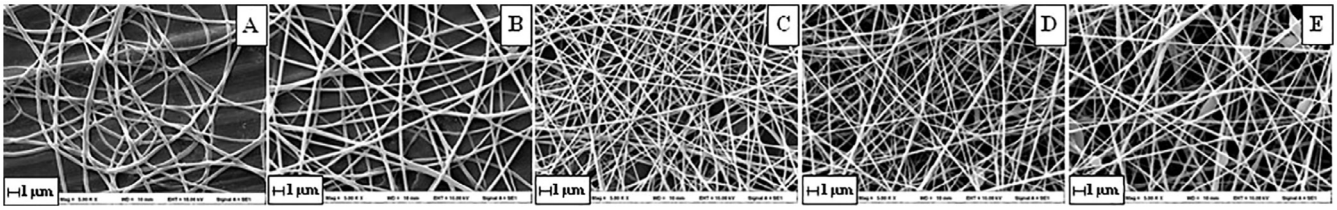

Fig. 5 – SEM images of the nanofibers prepared from polymer solutions containing 10% (w/w) PVA under applied voltages of (A) 5, (B) 10, (C) 15, (D) 20, and (E) 25 kV.

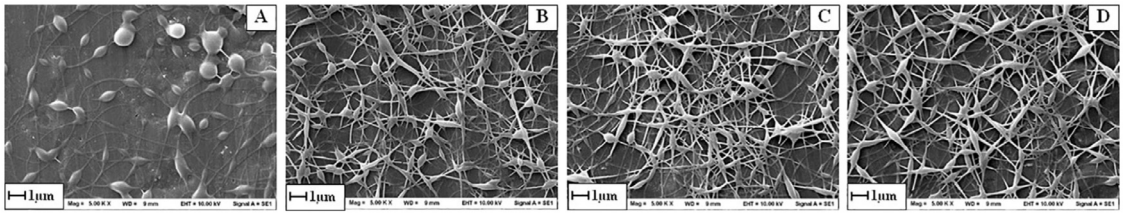

Fig. 6 – SEM images of nanofibers prepared from a polymer solution containing 5% (w/w) PVA and loaded with (A) 1%, (B) 1.5%, (C) 2.0%, and (D) 2.5% (w/w) clindamycin (applied voltage is 20 kV).

applied voltage to 25 kV increased the fiber diameter and resulted in bead formation. These results agree with the whipping model represented by Eq. (4), which indicates that a high electric current results in small fibers [18,19]. At an applied voltage of 5 kV, the nanofibers were flat and tended to fuse together (Fig. 5A). When the PVA concentration in the spraying solution was 10%, the feed rate did not affect the nanofiber appearance (data not shown); however, at 3% PVA, nanofibers were not obtained at feed rates of 0.5 ml/h and greater. The nanofiber products obtained at needle–collector distances ranging from 10 to 25 cm were similar.

Figs. 6 and 7 show SEM images of clindamycin-loaded nanofibers formed from solutions containing 5% and 10% PVA. For the drug-loaded nanofibers, the 5%-PVA formulation resulted in thick fibers with diameter 200–800 nm and comprising beads. For the PVA concentration of 10%, the diameters of the nanofibers loaded with 1.0%, 1.5%, 2.0%, and 2.5% clindamycin were 277.80 nm ± 27.05%, 263.24 nm ± 20.84%, 234.73 nm ± 20.84%, and 202.65 nm ± 26.45%, respectively. Thus, increase in the clindamycin content decreased the fiber diameter and inhibited bead formation. These results agree with the result of the three-dimensional equation describing the dynamics of electrospun jets that is suggested by Reneker et al. [20]:

$$\rho\frac{\partial\lambda fV}{\partial t} = \tau\frac{\partial P}{\partial s} + \lambda|k|Pn + \lambda|k|(\pi a\sigma - q_{el})n - \lambda e\frac{U_0}{h}k, \quad (5)$$

where λ is the geometric stretching ratio, f is the cross-sectional area, the subscript zero denotes time $t = 0$, ρ is the liquid density, V is the velocity vector, P is the longitudinal force in the jet cross section (of viscoelastic origin), $U0/h$ is the strength of the outer electric field, σ is the surface tension, k is the local curvature of the jet axis, e is the charge per unit jet length, qel is the net Coulomb force acting on a jet element from all the other elements depending on e, and the current overall configuration of the jet is the flux describing mass loss due to solvent evaporation from the jet surface. Based on Eq. (5), the cross-sectional area f is inversely related to the liquid density ρ. Consequently, increasing the concentration of loaded drug decreases the fiber diameter. In this study, the diameters of the drug-loaded fibers prepared from 10% PVA solution ranged from 200 to 300 nm (Fig. 6). Clindamycin crystals were not found in any of the formulations, indicating that the active drug was entrapped and dispersed in the polymer fibers.

3.3. *FTIR spectroscopy*

The FTIR spectra of the starting materials (PVA, gum, and clindamycin), their physical mixture, and a clindamycin-loaded PNP are illustrated in Fig. 8 . The FTIR spectrum of clindamycin HCl showed characteristic peaks at 1695 cm^{-1} (C = O stretching), 1090 and 1210 cm^{-1} (C–O stretching), 1561 cm^{-1} (C = C stretching), and 2940 cm^{-1} (C–H stretching) [21,22]. In the spectrum of PVA, the large bands observed at 3400 cm^{-1} are linked to O–H stretching. The vibrational band observed between 2840 and 3000 cm^{-1} corresponds to C–H stretching in alkyl groups, while the peaks between 1695 and 1745 cm^{-1} are attributed to C = O and C–O stretching in acetate groups [23]. The FTIR spectrum of gum showed characteristic absorption bands associated with –OH stretching vibration at 3500–3200 cm^{-1} and –CH stretching and bending vibrations at 2950–2800 cm^{-1} and around 1410 cm^{-1}, respectively. The absorption band appearing around 1600 cm^{-1} corresponds to the OH bonds of water molecules [24–26]. Peaks were observed at 1745, 1695, 1260, and 1090 cm^{-1} in the spectrum of the physical mixture (PM), similar to the peaks found in the spectrum of the starting materials. Comparing PM with PNP, the peaks around 2940 and 1100 cm^{-1} in the spectrum of PNP were broader. Most of the peaks in the PNP spectrum were quite similar to those in the PVA spectrum. However, the PNP spectrum also contained peaks corresponding to clindamycin at 1090 and 1255 cm^{-1}, indicating that the active drug was incorporated into the PNP without changing the chemical structure. Comparing to the starting material, the broader clindamycin peaks in PNP indicate that the drug might have converted into an amorphous form [27].

3.4. *Powder X-ray diffraction*

Fig. 9 shows the diffraction patterns of the starting materials (clindamycin HCl, gum, and PVA), their physical mixture, and a clindamycin-loaded PNP. The diffraction patterns of gum and PVA exhibited typical halo patterns indicating amorphous structures, whereas the pattern of clindamycin HCl revealed sharp crystalline peaks at 6.7°, 13.5°, 17.1°, and 37.9° [28]. These data suggested that clindamycin HCl was in a crystalline state, which explains the sharp endothermic melting peak in the DSC thermogram at 140 °C (Fig. 10). The diffraction pattern of the physical mixture demonstrated sharp peaks in locations similar to those in the pattern of the pure drug; however, these sharp peaks were not found in the pattern of the PNP,

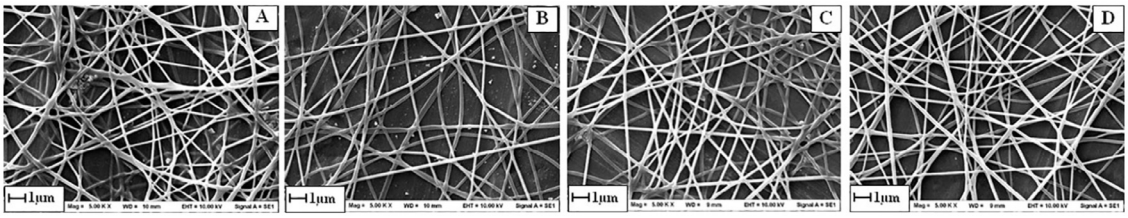

Fig. 7 – SEM images of nanofibers prepared from a polymer solution containing 10% (w/w) PVA and loaded with (A) 1%, (B) 1.5%, (C) 2.0%, and (D) 2.5% (w/w) clindamycin (applied voltage is 20 kV).

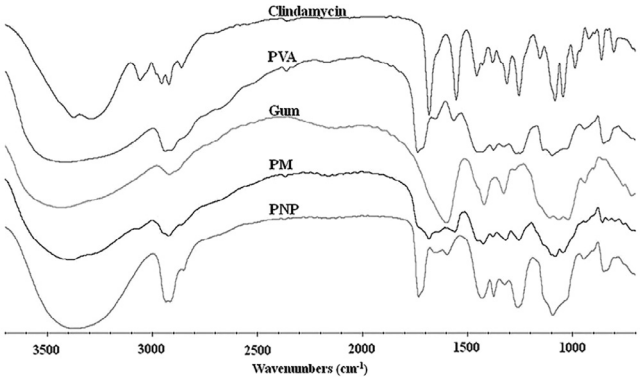

Fig. 8 – FTIR spectra of PVA, gum, clindamycin HCl, their physical mixture (PM), and the PNP loaded with 1% clindamycin HCl (PVA:gum = 9:1).

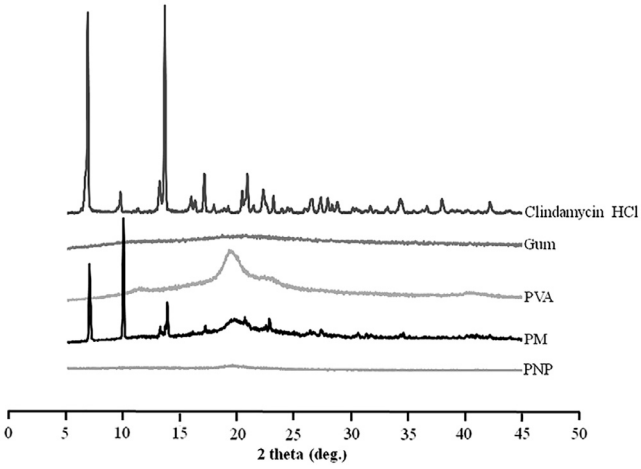

Fig. 9 – Powder X-ray diffraction patterns of clindamycin HCl, gum, PVA, their physical mixture (PM), and a PNP loaded with 1% clindamycin hydrochloride (PVA:gum = 9:1).

indicating that clindamycin HCl was molecularly dispersed in the polymers [27].

3.5. *Differential scanning calorimetry*

The DSC thermograms of clindamycin, PVA, gum, their physical mixture, and a PNP loaded with clindamycin are shown in Fig. 10. The thermogram of gum showed a broad endothermic peak at approximately 210 °C and a sharp degradation exothermic peak at 284 °C [14]. The DSC thermogram of clindamycin HCl showed a characteristic endothermic peak at 140 °C, which corresponds to the melting point of clindamycin HCl [29]. The thermogram of the PM exhibited broad endothermic peaks similar to those found in the thermogram of the PNP, possibly because the PM and PNP contained much larger amounts of polymer than clindamycin HCl. Therefore, the broad peak of the amorphous polymer in the PM and PNP covered the characteristic peak of clindamycin HCl.

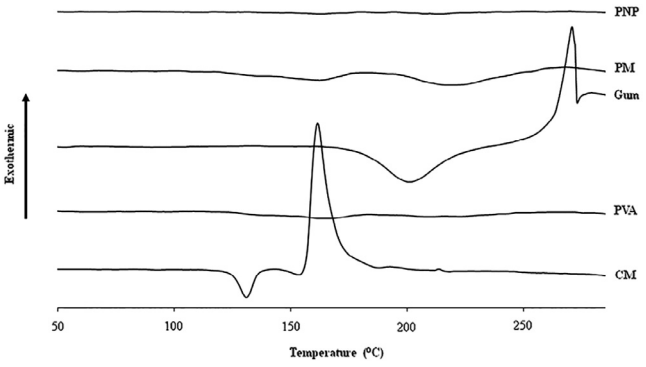

Fig. 10 – DSC thermograms of clindamycin HCl, gum, PVA, their physical mixture (PM), and a PNP loaded with 1% clindamycin HCl (PVA:gum = 9:1).

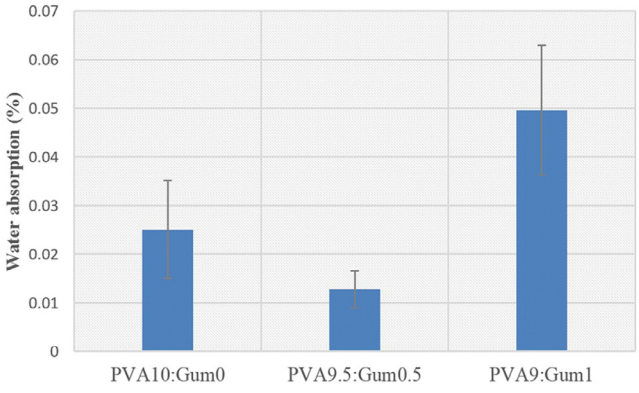

Fig. 11 – Water absorption percentages of the PNPs prepared from solutions with different PVA:gum ratios.

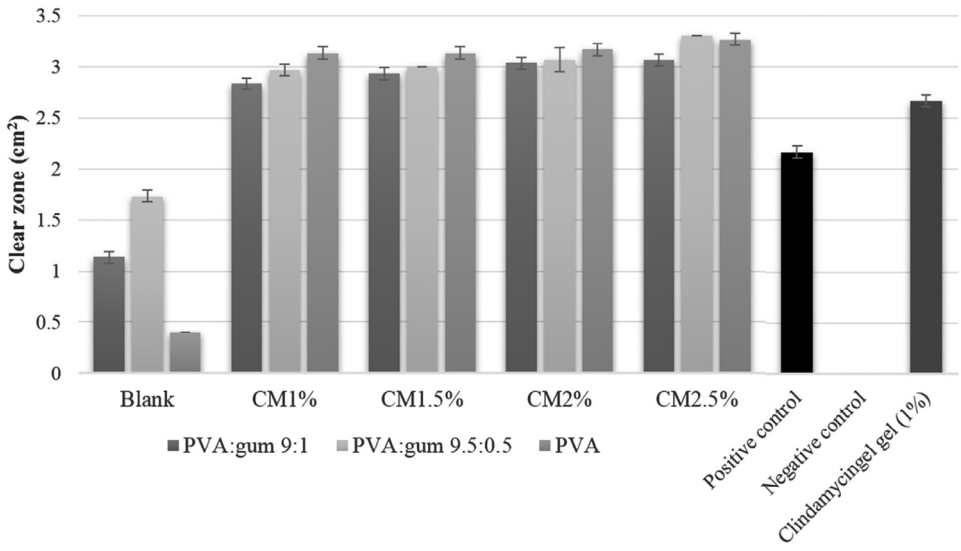

Fig. 12 – Average zones of *S. aureus* inhibition for PNPs without loaded drug, clindamycin (CM)-loaded PNPs, positive/negative controls, and clindamycin gel.

3.6. *Liquid absorption*

Fig. 11 shows the percentages of water absorption on films prepared from solutions with different PVA:gum ratios. The water-absorption percentages ranged from 0.012% to 0.05%, with the highest percentage obtained at a PVA:gum ratio of 9:1. This might be because adding an appropriate amount of the carboxymethylated gum can enhance the swelling of the PNP [30].

3.7. *Antimicrobial studies*

The antibacterial activities of PNPs loaded with clindamycin HCl were evaluated against *S. aureus* using disk-diffusion tests (Fig. 12). The PNP without loaded drug did not exhibit any bactericidal activity; in contrast, the PNPs loaded with 1.0%–2.5% clindamycin HCl showed excellent bactericidal activity (Fig. 10), with the antibacterial activity being slightly dependent on clindamycin content. The antibacterial activities of the drug-loaded PNPs were significantly greater than that of 1% clindamycin gel. These results agree with the report of Unnithan et al., who concluded that interconnected nanofibers create perfect blocks and pores in the membrane, thereby preventing bacterial penetration and effectively avoiding exogenous infections [31]. The results indicate that the fabricated PNPs are good antibacterial membranes and can be applied as wound dressings.

4. Conclusion

In this study, EHDA was applied to fabricate PNPs loaded with clindamycin. The effects of the characteristics of the spraying solution and the instrument parameters on the EHDA products were examined. Round nanofibers with smooth surfaces and an average diameter of 163.86 nm were obtained from a precursor solution of 10% PVA (w/w) in methanol under an applied voltage of 20 kV. The addition of tamarind seed gum at a PVA:gum ratio of 9:1 enhanced fluid absorption on the PNP. Finally, clindamycin was successfully loaded in the PNPs, and the drug-loaded PNPs exhibited good antibacterial activity. The findings indicate that the new drug-loaded PNPs fabricated via EHDA have the potential to be applied as wound-dressing materials.

Conflict of interest

The authors declare that there are no conflicts of interest.

Acknowledgement

The authors acknowledge the Faculty of Pharmaceutical Sciences, Burapha University for financial support (grant numbers 9/2558). The assistance of Ms. Kwanchanok Tabpara and Ms. Kamonchanok Wangjit on laboratory work is greatly appreciated.

REFERENCES

[1] Nguyen R, Su J. Treatment of acne vulgaris. Paediatr. Child Health 2011;21:119–25.
[2] White GM. Recent findings in the epidemiologic evidence, classification, and subtypes of acne vulgaris. J Am Acad Dermatol 1998;39(2 Pt 3):S34–7.
[3] Lee TW, Kim JC, Hwang SJ. Hydrogel patches containing triclosan for acne treatment. Eur J Pharm Biopharm 2003;56:407–12.
[4] Zaenglein AL, Pathy AL, Schlosser BJ, et al. Guidelines of care for the management of acne vulgaris. J Am Acad Dermatol 2016;74:945–73 e33.
[5] Jones V, Grey JE, Harding KG. Wound dressings. Br Med J 2006;332:777–80.

[6] Kahraman E, Güngör S. Polymeric micellar nanocarriers of benzoyl peroxide as potential follicular targeting approach for acne treatment. Colloids Surf B Biointerfaces 2016;146:692–9.
[7] Vijayan V, Aafreen S, Sakthivel S, Reddy KR. Formulation and characterization of solid lipid nanoparticles loaded Neem oil for topical treatment of acne. J Acute Dis 2013;2:282–6.
[8] Jain AK, Jain A, Garg NK, et al. Adapalene loaded solid lipid nanoparticles gel: an effective approach for acne treatment. Colloids Surf B Biointerfaces 2014;121:222–9.
[9] Shen X, Yu D, Zhu L, Branford-White C, White K, Chatterton NP. Electrospun diclofenac sodium loaded Eudragit L 100-55 nanofibers for colon-targeted drug delivery. Int J Pharm 2011;408:200–7.
[10] Kenawy ER, Bowlin GL, Mansfield K, Layman J, Simpson DG, Sanders EH. Release of tetracycline hydrochloride from electrospun poly(ethylene-co-vinylacetate), poly(lactic acid), and a blend. J Control Release 2002;81:57–64.
[11] Xie J, Jiang J, Davoodi P, Srinivasan MP, Wang CH. Electrohydrodynamic atomization: a two-decade effort to produce and process micro-/nanoparticulate materials. Chem Eng Sci 2015;125:32–57.
[12] Kamoun EA, Kenawy E-RS, Chen X. A review on polymeric hydrogel membranes for wound dressing applications: PVA-based hydrogel dressings. J Adv Res 2017;8:217–33.
[13] Yadav I, Rathnam VS, Yogalakshmi Y, et al. Synthesis and characterization of polyvinyl alcohol-carboxymethyl tamarind gum based composite films. Carbohydr Polym 2017;165(Suppl.C):159–68.
[14] Huanbutta K, Sangnim T, Sittikijyothin W. Physicochemical characterization of gum from tamarind seed: potential for pharmaceutical application. Asian J Pharm Sci 2016;11:176–7.
[15] Gong H, Liu M, Chen J, Han F, Gao C, Zhang B. Synthesis and characterization of carboxymethyl guar gum and rheological properties of its solutions. Carbohydr Polym 2012;88:1015–22.
[16] Huanbutta K, Sangnim T, Limmatvapirat S, Nunthanid J, Sriamornsak P. Design and characterization of prednisolone-loaded nanoparticles fabricated by electrohydrodynamic atomization technique. Chem Eng Res Des 2016;109:816–23.
[17] Rub MA, Azum N, Asiri AM, Alfaifi SY, Alharthi SS. Interaction between antidepressant drug and anionic surfactant in low concentration range in aqueous/salt/urea solution: a conductometric and fluorometric study. J Mol Liq 2017;227(Suppl.C):1–14.
[18] Rafiei S, Maghsoodloo S, Noroozi B, Mottaghitalab V, Haghi AK. Mathematical modeling in electrospinning process of nanofibers: a detailed review. Cellul Chem Technol 2012;47:323–38.
[19] Hohman MM, Shin M, Rutledge G, Brenner MP. Electrospinning and electrically forced jets. II. Applications. Phys Fluids 2001;13:2221–36.
[20] Reneker DH, Yarin AL, Fong H, Koombhongse S. Bending instability of electrically charged liquid jets of polymer solutions in electrospinning. J Appl Phys 2000;87(9 I):4531–47.
[21] Patel P, Patel P. Formulation and evaluation of clindamycin HCL in situ gel for vaginal application. Int J Pharm Investig 2015;5:50–6.
[22] Mohamed AI, Abd-Motagaly AM, Ahmed OA, Amin S, Mohamed Ali AI. Investigation of drug-polymer compatibility using chemometric-assisted UV-spectrophotometry. Pharmaceutics 2017;9:7.
[23] Mansur HS, Sadahira CM, Souza AN, Mansur AA. FTIR spectroscopy characterization of poly (vinyl alcohol) hydrogel with different hydrolysis degree and chemically crosslinked with glutaraldehyde. Mater Sci Eng C 2008;28:539–48.
[24] Banegas RS, Zornio CF, Borges AD, Porto LC, Soldi V. Preparation, characterization and properties of films obtained from cross-linked guar gum. Polímeros 2013;23:182–8.
[25] Rajput G, Pandey IP, Joshi G. Carboxymethylation of Cassia angustifolia seed gum: synthesis and rheological study. Carbohydr Polym 2015;117:494–500.
[26] Huanbutta K, Sangnim T, Sittikijyothin W. Development of tamarind seed gum as dry binder in formulation of diclofenac sodium tablets. Walailak J Sci Tech 2016;13:863–74.
[27] Huanbutta K, Sriamornsak P, Luangtana-anan M, et al. Application of multiple stepwise spinning disk processing for the synthesis of poly(methyl acrylates) coated chitosan–diclofenac sodium nanoparticles for colonic drug delivery. Eur J Pharm Sci 2013;50:303–11.
[28] Daihom B, Alayoubi A, Ma D, et al. Development and physicochemical characterization of clindamycin resinate for taste masking in pediatrics. Drug Dev Ind Pharm 2016;42:1600–8.
[29] Rauta PR, Das NM, Nayak D, Ashe S, Nayak B. Enhanced efficacy of clindamycin hydrochloride encapsulated in PLA/PLGA based nanoparticle system for oral delivery. IET Nanobiotechnol 2016;10:254–61.
[30] Ponnikornkit B, Ngamsalak C, Huanbutta K, Sittikijyothin W. Swelling behaviour of carboxymethylated tamarind gum. Adv Mater Res 2015;1060:137–40.
[31] Unnithan AR, Barakat NA, Pichiah PT, et al. Wound-dressing materials with antibacterial activity from electrospun polyurethane–dextran nanofiber mats containing ciprofloxacin HCl. Carbohydr Polym 2012;90:1786–93.